Am J Physiol Renal Physiol 294: F1238–F1248, 2008.
First published March 5, 2008; doi:10.1152/ajprenal.00326.2007.

Mesenchymal transition in kidney collecting duct epithelial cells

Larissa Ivanova, Michael J. Butt, and Douglas G. Matsell

Department of Pediatrics and Child and Family Research Institute, British Columbia Children's Hospital, Vancouver, British Columbia, Canada

Submitted 14 July 2007; accepted in final form 28 February 2008

Ivanova L, Butt MJ, Matsell DG. Mesenchymal transition in kidney collecting duct epithelial cells. *Am J Physiol Renal Physiol* 294: F1238–F1248, 2008. First published March 5, 2008; doi:10.1152/ajprenal.00326.2007.—Progressive organ damage due to tissue scarring and fibrosis is a paradigm shared by numerous human diseases including chronic kidney disease. The purpose of this study was to confirm the hypothesis that collecting duct (CD) epithelial cells can undergo mesenchymal transition (EMT) in vitro. The mechanism by which CDs undergo EMT is complex and involves both early and late cellular events. Early events include rapid insulin-like growth factor (IGF)-induced Akt and GSK-3β phosphorylation, associated with early disruption of E-cadherin-β-catenin membrane colocalization, with translocation of E-cadherin to endosomes, with translocation of β-catenin to the nucleus, and with an increase in Snail expression. Transforming growth factor-β1, on the other hand, induced early activation of Smad3 and its translocation to the nucleus, Erk1/2 phosphorylation, and early disruption of membrane E-cadherin localization. The late consequences of these events included a phenotypic transformation of the cells to a mesenchymal morphology with associated increase in vimentin and α-smooth muscle actin protein expression and a decrease in total cellular E-cadherin expression, detectable as early as 24 h after stimulation.

epithelial-mesenchymal transition; insulin-like growth factor-I; E-cadherin

PROGRESSIVE ORGAN DAMAGE due to tissue scarring and the development of fibrosis is a paradigm shared by many human diseases including chronic kidney disease.

Interstitial fibrosis is the common end point for a number of kidney disorders and is seen in many of the forms of glomerulonephritis and in urinary tract obstruction (12, 35, 36, 54). In fact, the severity of interstitial fibrosis early in the clinical presentation of most of these diseases predicts the ultimate prognosis and likelihood of progression of disease (11, 27, 44, 50).

Interstitial fibroblasts are the principal effector cells of organ fibrosis, and their origin has traditionally thought to be from proliferating resident fibroblasts or from circulating marrow stromal cell progenitors. Elegant studies using bone marrow chimeras and transgenic reporter mice, however, have demonstrated that up to 36% of interstitial fibroblasts in postnatal ureteric obstructed kidneys were derived from tubular epithelia (18).

Descriptive studies in humans have supported the hypothesis that the injured tubular epithelium is an important source of interstitial mesenchymal cells associated with fibrosis (19, 37, 42). Immunohistochemical studies of renal biopsies from adult patients with a variety of underlying renal diseases associated with interstitial fibrosis demonstrate the expression of mesenchymal proteins such as smooth muscle actin (SMA) and vimentin in tubular epithelial cells, including those of collecting ducts (CDs), adjacent to regions of interstitial fibrosis and tubular basement membrane disruption. Similarly, we have demonstrated (28, 30) marked alterations in normal tubular epithelial cell differentiation, interstitial fibrosis, and marked expansion of the mesenchymal compartment in a number of human fetal kidney disorders, including obstructive renal dysplasia. In a unique nonhuman primate fetal model of unilateral ureteric obstruction we previously demonstrated (52) significant CD epithelial-to-mesenchymal phenotypic changes and the migration of transitioning cells into the periductular fibromuscular collars. These data support the possibility that cells from obstructed CDs undergo epithelial-mesenchymal transition (EMT) and are an important source of the infiltrating interstitial mesenchymal cells seen in fetal urinary tract obstruction.

A number of soluble growth factors, cytokines, and extracellular proteins have been shown to affect EMT and to influence disease progression. Transforming growth factor (TGF)-β1, however, appears to play a prominent role, with an increase in expression almost universally in progressive forms of renal disease (3, 26, 55). In addition, in a number of cell systems this peptide has the demonstrated ability to drive cells through all the key steps of EMT, including loss of cell adhesion, de novo SMA expression, disruption of the tubular basement membrane, and enhanced cell migration (1, 49, 55). While the role of Smad pathway activation in TGF-β1-induced EMT and fibrosis is well established, the role of noncanonical signaling in this process, through activation of receptor tyrosine kinases, has been underappreciated.

Growth factors such as the insulin-like growth factors (IGFs) act in concert with TGF-β1 to invoke EMT. Both IGF-I and IGF-II are small-molecular-weight peptides that interact with both IGF-I and IGF-II receptors (IGF-1R, IGF-2R) but transduce most of their biological effects through IGF-1R. Their biological activities are modulated by a group of binding proteins. IGFs and the IGF-1R are expressed in both the developing and mature kidney (31) and have demonstrated roles in development, in cell survival (6), and in the maintenance of glomerular integrity (5). Marked alterations in IGF expression have been observed in various renal diseases characterized by overexpression of TGF-β1 and expansion of the mesenchymal compartment and fibrosis including multicystic renal disease, lupus glomerulonephritis (32), Wilms tumor (2), and diabetic nephropathy (51). While the expression of IGFs in kidneys undergoing fibrosis is altered, particularly in areas of

Address for reprint requests and other correspondence: D. G. Matsell, Dept. of Pediatrics, Div. of Nephrology, British Columbia Children's Hospital, K4-150, 4480 Oak St., Vancouver, BC, Canada V6H 3V4 (e-mail: dmatsell@cw.bc.ca).

The costs of publication of this article were defrayed in part by the payment of page charges. The article must therefore be hereby marked "*advertisement*" in accordance with 18 U.S.C. Section 1734 solely to indicate this fact.

active tubular injury (29), the role of IGFs in EMT in the kidney has been largely unexplored. The purpose of this study was to determine the ability of IGF-I and TGF-β1 to induce CD epithelial cells to undergo EMT, and to characterize the intracellular signaling mechanisms that underlie this transition.

MATERIALS AND METHODS

Reagents and antibodies. Cell culture reagents, media, and serum were obtained from GIBCO BRL (Burlington, ON, Canada). Electrophoresis reagents were purchased from Bio-Rad (Mississauga, ON, Canada). The protease inhibitors orthovanadate and phenylmethylsulfonyl fluoride were purchased from Sigma-Aldrich Canada (Oakville, ON, Canada) and leupeptin, aprotinin, and pepstatin from Boehringer Mannheim. Monoclonal antibodies (MAbs) against E-cadherin were ordered from BD Transduction Laboratories (San Diego, CA), and MAb against glyceraldehyde-3-phosphate dehydrogenase (GAPDH), SMA, vimentin, and rabbit polyclonal antibodies (Abs) against TGF-β1, specific inhibitor of Smad3 (SIS3), and LY-294002 were purchased from Sigma-Aldrich Canada. Polyclonal Abs against total and phosphorylated Akt, Erk1/2, Smad2, Smad3, glycogen synthetase kinase (GSK)-3α/β, Smad2/3, and also against β-catenin and cAMP response element binding protein (CREB; 48H2) were obtained from Cell Signaling Technology. MAb against vinculin was obtained from Upstate Cell Signaling Solutions. Goat anti-rabbit Alexa 488 and Alexa 568 and goat-anti-mouse Alexa 488 and Alexa 568 antibodies were from Invitrogen Molecular Probes and Sigma-Aldrich Canada. Rabbit Ab to fibronectin was obtained from Santa Cruz Biotechnology. Anti-mouse and anti-rabbit IgG horseradish peroxidase (HRP)-linked secondary Abs were purchased from Jackson ImmunoResearch Laboratories (West Grove, PA), and enhanced chemiluminescence (ECL) reagents were from Sigma-Aldrich Canada. IGF-I and TGF-β1 were obtained from Upstate Cell Signaling Solutions. Prolong* Gold antifade reagent with DAPI was from Invitrogen Molecular Probes. All other reagents were from Sigma-Aldrich Canada.

Cell culture and treatments. The mouse inner medullary CD cell line mIMCD3 was used in these experiments. This line is derived from an SV40 transgenic mouse as described elsewhere (43) and was obtained from the American Type Culture Collection (Manassas, VA). Cells were maintained in Ham's F-12 medium-Dulbecco's modified Eagle's medium (1:1) supplemented with 10% FBS, penicillin (100 U/ml), and streptomycin (100 μg/ml) (Life Technologies, Burlington, ON, Canada) at 37°C in a humidified incubator with 5% CO_2. The medium was changed every other day. Before stimulation with growth factors, cells were incubated in serum-free medium for 18–24 h.

Western Blot analysis. mIMCD3 cells were harvested in each experiment by scraping into 2 ml of chilled PBS and pelleting in a 15-ml conical tube at 500 rpm for 5 min. Cells were then lysed in buffer containing (in mM) 150 NaCl, 25 HEPES pH 7.4, 1 EGTA, 5 EDTA, 1 sodium orthovanadate, 50 NaF, and 1 phenylmethylsulfonyl fluoride, with 1% (vol/vol) NP-40, 0.25% (wt/vol) sodium deoxycholate, and 10 μg/ml aprotinin, leupeptin, and pepstatin. The lysates were clarified by centrifugation at 16,000 *g* and 4°C for 20 min, and the protein concentration was determined by the Micro-BCA Protein Assay Kit (Pierce Biotechnology) according to the manufacturer's instructions. Cellular proteins were separated by SDS-PAGE, transferred onto a nitrocellulose membrane, and probed with the appropriate antibodies, followed by incubation with HRP-conjugated secondary antibodies. Detection was carried out with ECL (ECL kit, Sigma-Aldrich Canada). Cytosolic vinculin and nuclear Creb proteins were used as control for cytosolic and nuclear protein loading. Densitometry of the blots was performed with Quantity One software (Bio-Rad), and results were normalized to the signal obtained by Western blotting of total proteins or GAPDH in the same cell samples.

Immunoprecipitation. mIMCD3 cells grown to confluence on 100-mm dishes with or without treatment were washed twice in ice-cold PBS and solubilized in cold RIPA buffer containing protease inhibitors. The Micro-BCA Protein Assay Kit was used to quantify the total protein concentration. One hundred microliters of supernatant containing 500 μg of total protein were precleaned for 1 h at 4°C with G-Sepharose beads. Precleaned lysates were centrifuged, and supernatants were incubated with 2.5 μg of monoclonal anti-E-cadherin and polyclonal anti-β-catenin Abs at 4°C overnight. Fifty microliters of 50% G-Sepharose beads was added to each tube, and incubation proceeded at 4°C for 2 h. Immunoprecipitated complexes were collected by centrifugation for 30 s at 10,000 rpm, washed three times in immunoprecipitation buffer, resuspended in 2× sample buffer, and analyzed by SDS-PAGE and immunoblotting.

Subcellular fractionation. Subcellular fractionated protein was extracted from mIMCD3 cells. After washing in ice-cold PBS, cells were resuspended in a 5-ml volume of *buffer A* [in mM: 10 HEPES (pH 7.9), 1.5 $MgCl_2$, and 0.5 mM DTT with the protease inhibitors] and incubated for 10 min on ice. The cells were then passed through a 22-gauge needle 10 times and centrifuged for 2 min at 10,000 rpm and 4°C, and the supernatant was designated the cytoplasmic protein fraction. The nuclear protein fraction was extracted as described by Dignam et al. (10). The pellets (crude nuclei) were rinsed in *buffer B* [in mM: 10 Tris·HCl (pH 7.2), 2 $MgCl_2$], resuspended in *buffer C* [in mM: 20 mM HEPES (pH 7.9), 1.5 $MgCl_2$, 0.2 EDTA, and 0.5 DTT, with 20% (vol/vol) glycerol, 0.42 M NaCl, and protease inhibitors], and incubated for 30 min on ice while vortexing for 30 s at 10-min intervals. Nuclei were ruptured by passing through a 26-gauge needle 10 times and incubated for another 10 min on ice. Nuclear debris was pelleted by centrifuging for 20 min at 13,000 rpm and 4°C and then frozen on dry ice at −80°C. The resulting supernatant was considered to be the nuclear protein fraction. Protein concentrations were subsequently determined with the Micro-BCA Protein Assay Kit.

Immunocytochemistry. mIMCD3 cells were seeded and grown on glass coverslips. For immunofluorescence assays, cells were fixed with 4% formaldehyde for 15 min, permeabilized with 0.1% Triton X-100 for 10 min, and washed with PBS. Coverslips were blocked with 5% normal serum in PBS-Triton X-100 from the same species as the secondary Ab for 60 min and then incubated overnight at 4°C with various combinations of the primary Abs. Coverslips were then washed with PBS-Tween 20 for 20 min, followed by a 1-h incubation with the appropriate fluorescent dye-conjugated secondary Ab. Coverslips were mounted with Prolong* Gold antifade reagent with DAPI on glass slides and observed with a Leica DM4000B microscope and appropriate filters.

Cell transfection. Subconfluent mIMCD3 cells grown on coverslips were transfected with the green fluorescent protein construct GFP-Rab5 (generously provided by Dr. M. Metzler, University of British Columbia, Vancouver, Canada) (9) and the FuGENE6 transfection reagent (Roche). Cells were then washed in PBS, fixed, and stained with appropriate Abs. Coverslips were mounted onto slides with Prolong* Gold antifade reagent with DAPI and observed with a Leica DM4000B microscope and appropriate filters.

RESULTS

Cell density dependence of E-cadherin/β-catenin expression in mIMCD3 cells. The E-cadherin-β-catenin complex plays a major role in epithelial cell-cell adhesion, morphogenesis, and maintenance (14). Before studying the effects of IGF-I and TGF-β1 on the integrity of E-cadherin-β-catenin complexes in mIMCD3 cells, we analyzed how cell monolayer confluence influences protein expression and distribution. In sparse subconfluent cell culture, β-catenin localized to the cell periphery and cell membrane (Fig. 1*A*), while the adherens junction protein E-cadherin localized diffusely in the cytoplasm. In confluent cells cultured for 24 h, β-catenin localized predominantly to the cell membrane. E-cadherin localized mainly in

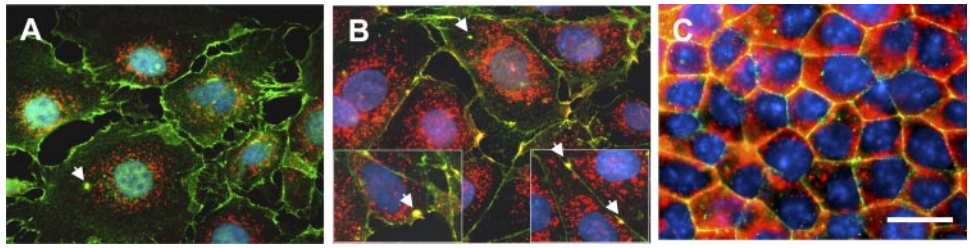

Fig. 1. E-cadherin and β-catenin expression is dependent on confluence of the culture monolayer and the length of time in culture. *A*: subconfluent cells (50% confluent) show cytoplasmic and perinuclear distribution of E-cadherin (red) and diffuse cytoplasmic and nuclear localization of β-catenin (green). *B*: with an increase in monolayer confluence (80–100% at 24 h in culture) E-cadherin distributes to the cytoplasm and also colocalizes with β-catenin to the cell membrane (yellow and arrowheads), while β-catenin is now predominantly distributed to the cell membrane. Arrowheads indicate E-cadherin-β-catenin complexes. *C*: with an increase in monolayer confluence and time in culture (100% confluence at 72 h in culture), E-cadherin distributes more to the cell membrane, colocalizing with β-catenin (yellow). Scale bar, 10 μm.

the cell cytoplasm, with some accumulation and colocalization with β-catenin on cell extensions and at focal contacts (Fig. 1*B*). In late confluent monolayers, β-catenin and E-cadherin colocalized at cell-cell boundaries, with cytoplasmic expression of E-cadherin (Fig. 1*C*).

Phenotypic changes in CD epithelial cells. Stimulation of mIMCD3 cell monolayers by both IGF-I and TGF-β1, separately and together, resulted in a significant change in morphology, as demonstrated by phase-contrast microscopy, with transition from a typical cobblestone morphology to areas of cells with mesenchymal spindle-shaped and fusiform features (Fig. 2, *A*, *F*, and *K*). These morphological changes were associated with the acquisition of other mesenchymal characteristics, including an increase in vimentin (Fig. 2, *B*, *G*, and *L*) and SMA (Fig. 2, *C*, *H*, and *M*) expression, with the loss of epithelial characteristics including E-cadherin expression (Fig. 2, *D*, *I*, and *N*) and with an increased expression of the matrix protein fibronectin (Fig. 2, *E*, *J*, and *O*). The morphological changes were apparent as early as 24 h of incubation, coincident with the changes seen on Western blot analysis. The cells undergoing conformational changes were the same cells that exhibited an increase in the expression of vimentin and SMA. These growth factor-induced phenotypic changes were associated with corresponding changes in the quantity of protein expression over time, as demonstrated by Western blot analysis for vimentin, SMA, and E-cadherin of protein extracted from the monolayers (Fig. 3).

While the effects of TGF-β1 on these CD cells were not entirely surprising, these results demonstrate, for the first time, the ability of IGF-I to induce EMT in kidney epithelial cells. When mIMCD3 cells were incubated with both IGF-I and TGF-β1 there were no significant changes in the extent of mesenchymal transition. By Western blot analysis, coincubation did not appear to increase total cell vimentin and SMA expression nor decrease E-cadherin more than with TGF-β1 stimulation alone (Fig. 3, *B* and *C*).

Disruption of E-cadherin/β-catenin colocalization. To begin to study the early effects of IGF-I and TGF-β1 on the induction of EMT in mIMCD3 cells, we studied the changes in expression and localization of E-cadherin and β-catenin. IGF-I stim-

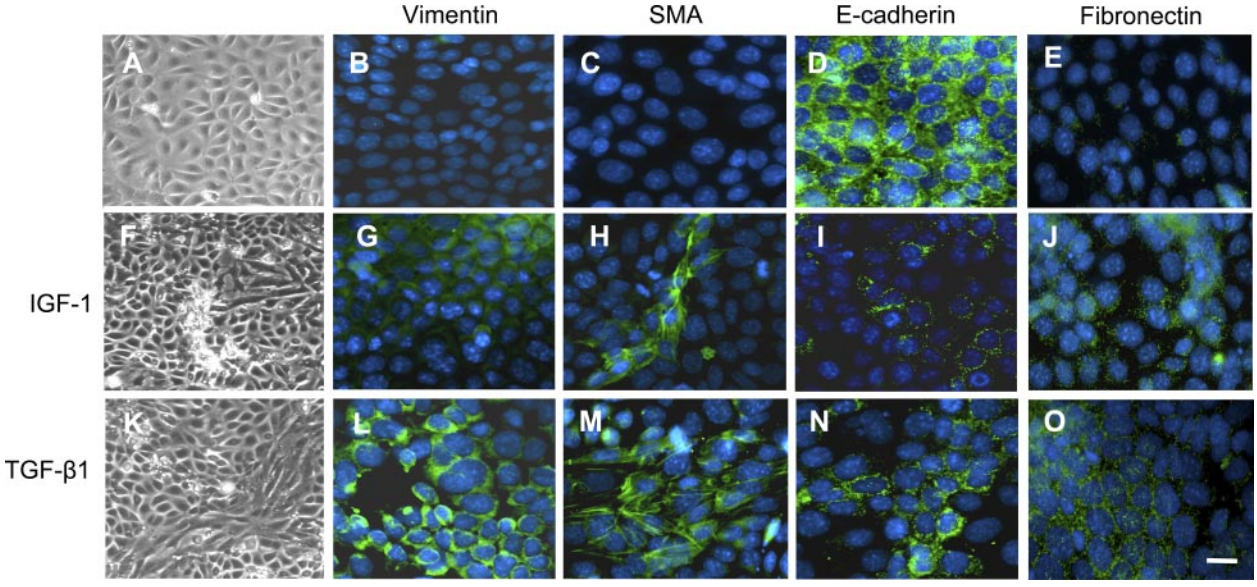

Fig. 2. Induction of mIMCD3 epithelial-mesenchymal transition (EMT). mIMCD3 cells were grown on glass coverslips for 24 h, starved for 20 h, and then incubated for an additional 72 h with 10 ng/ml insulin-like growth factor (IGF)-I (*F–J*) or with 10 ng/ml transforming growth factor (TGF)-β1 (*K–O*). Compared with control cells (*A–E*), stimulated cells displayed an altered mesenchymal morphology by phase-contrast microscopy (*F*, *K*), with de novo expression of vimentin (*G*, *L*) and smooth muscle actin (SMA; *H*, *M*), a redistribution and decreased expression of E-cadherin (*I*, *N*), and an increase in fibronectin expression (*J*, *O*) by immunofluorescence microscopy. Scale bar, 10 μm.

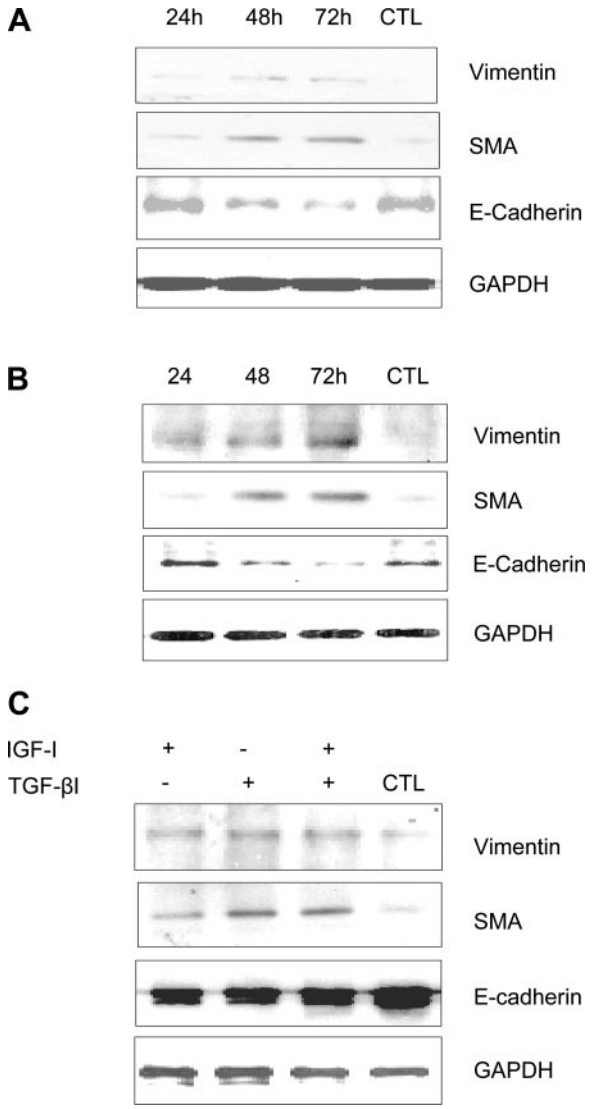

Fig. 3. Induction of mIMCD3 EMT: Western blot analysis of total cell protein of stimulated mIMCD3 cells confirming immunohistochemistry results. Stimulation of mIMCD3 cells by IGF-I (10 ng/ml; *A*) and by TGF-β1 (10 ng/ml; *B*) for 24, 48, and 72 h resulted in an increase in vimentin and SMA protein expression with a corresponding decrease in E-cadherin expression evident after 24 h of stimulation. *C*: stimulation by IGF-I (10 ng/ml), TGF-β1 (10 ng/ml), and a combination of both factors for 72 h resulted in a significant increase in vimentin and SMA expression with a decrease in E-cadherin expression. Results were more pronounced with TGF-β1 stimulation. CTL, control.

ulation for 30 min rapidly induced translocation of E-cadherin from adherens junction to perinuclear cytoplasmic vesicles (Fig. 4*B*), with no changes in total cell E-cadherin protein content as determined by Western blot analysis (data not shown). The nature of these vesicles was confirmed by labeling cells with an Ab to E-cadherin in GFP-rab5-transfected cells and by double labeling of cells with Abs to E-cadherin and to rab5, a key regulator of transport from the plasma membrane to early endosomes (9) (Fig. 4, *D–I*). In both circumstances, the vesicular staining pattern of E-cadherin partially overlapped with rab5 expression, indicating that with IGF stimulation E-cadherin accumulates in early endosomal or recycling compartments.

In control, unstimulated mIMCD3 cells, β-catenin was localized primarily to cell-cell contacts or intercellular junctions, colocalizing as expected with E-cadherin (Figs. 1*B* and 4*A*). Early stimulation of cells with IGF-I resulted in translocation of β-catenin from the membrane to the cytoplasm and to the nucleus (Fig. 4*B*). This nuclear expression of β-catenin was demonstrated by Western blot analysis of fractionated cellular protein, with no changes in total cell β-catenin content (Fig. 4*J*).

In cells stimulated with TGF-β1, as with IGF-I, E-cadherin was rapidly translocated from adherens junction to cytoplasmic endosomes. In contrast to IGF-I stimulation, TGF-β1 stimulation resulted in β-catenin expression remaining robust and exclusive to the cell membrane (Fig. 4*C*).

To further analyze the effect of TGF-β1 and IGF-I on the dynamic integrity of the E-cadherin-β-catenin complex we immunoprecipitated E-cadherin from total protein extracted from untreated and treated mIMCD3 cells at different time points. After IGF-I or TGF-β1 stimulation, at both 1 and 72 h, there was a reduction of E-cadherin-associated β-catenin expression in treated cells, more marked with the TGF-β1 treatments (Fig. 4*K*). These results show that stimulation of mIMCD3 cells with IGF-I and TGF-β1 not only decreases the level of expression of junctional proteins but also causes the disassembly of the E-cadherin-β-catenin complexes.

IGF-I signaling. To identify potential mechanisms by which IGF-I induces EMT we studied its effect on mIMCD3 intracellular signaling. Stimulation of cells with IGF-I alone at a concentration of 10 ng/ml resulted in an expected rapid phosphorylation of Akt, as has been previously demonstrated in other cell types (Fig. 5*A*). Examination of cellular fractions revealed that this activation was associated with a rapid increase in phosphorylation of both cytosolic and nuclear Akt, with the majority of phospho (p)-Akt present in the nuclear fraction after 5 min of IGF stimulation (Fig. 6*A*). Interestingly, the nuclear and cytoplasmic Akt species migrated differently on Western blot analysis, with the larger nuclear species suggesting the possibility of phosphorylation of a different Akt species directly within the nucleus. These effects were both dose- and time dependent (data not shown). As expected, we noted a similar phenomenon for GSK-3β, a well-characterized target of activated Akt, which underwent rapid phosphorylation and nuclear translocation on stimulation of the cells with IGF (Fig. 5*A*). IGF stimulation of the monolayers did not result in any significant Erk1/2 or Smad3 phosphorylation (data not shown).

TGF-β1 signaling. As with IGF-I, we studied the early intracellular signaling events induced by TGF-β1 in mIMCD3 cells. As expected, TGF-β1 mediated its effects primarily through activation of the intracellular Smad pathway, with a rapid time- and dose-dependent phosphorylation of Smad3 with an approximately threefold increase in phosphorylation as early as 15 min after stimulation (Fig. 5*B*). Examination of Smad3 dynamics revealed a rapid increase in both nuclear and cytoplasmic phosphorylated Smad3, with a disappearance of cytoplasmic Smad3 by 3 h of stimulation, suggesting a rapid translocation to the nucleus (Fig. 6*B*). TGF-β1 stimulation of the monolayers resulted in a similar but less robust increase in Smad2 phosphorylation (Fig. 5*B*). In addition to the expected increase in Smad activation, with TGF-β1 stimulation there was a rapid decrease in Akt phosphorylation suggesting a decrease in phosphatidylinositol 3-kinase (PI3-kinase) pathway activation. Additionally, there was a significant increase in

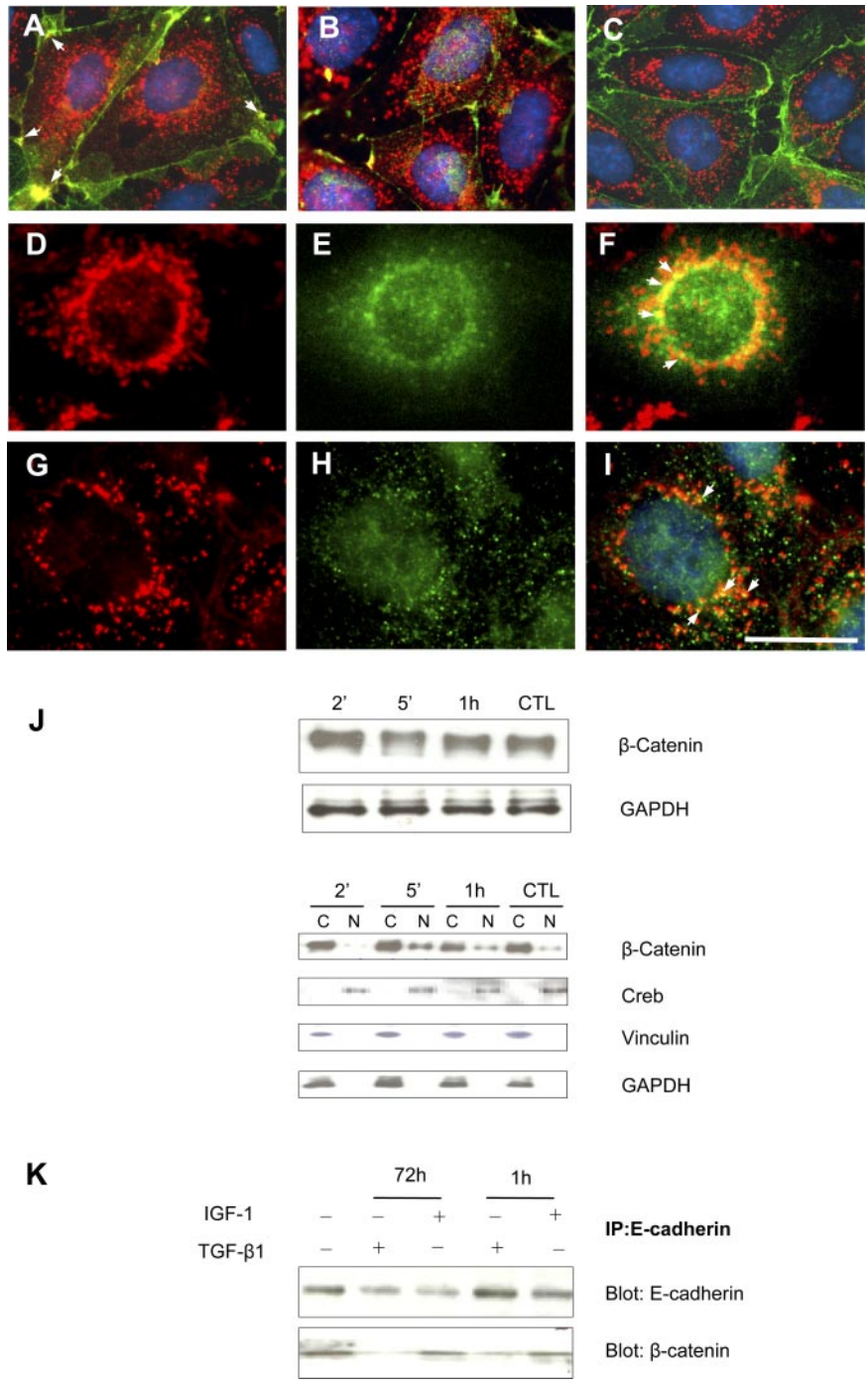

Fig. 4. IGF-induced disruption of β-catenin-E-cadherin complexes. mIMCD3 cells were grown on glass coverslips for 24 h, starved for 20 h, and then incubated with 10 ng/ml IGF-I or TGF-β1 for 30 min. *A*: control cell monolayers demonstrated cell membrane colocalization (yellow) of E-cadherin (red) and β-catenin (green) immunoreactivity (arrowheads), particularly at points of focal adhesion. *B*: in cells stimulated with IGF-I, both E-cadherin and β-catenin localized to the cytoplasm and nucleus, while at the cell membrane there was only faint β-catenin expression. *C*: in cells stimulated with TGF-β1, E-cadherin expression was restricted to the cytoplasm, while β-catenin expression was robust and exclusive to the cell membrane. Green fluorescent protein (GFP)-rab5-transfected cells stimulated with IGF-I demonstrate expression of E-cadherin (red; *D*), GFP-rab5 (green; *E*), and their colocalization (yellow and arrowheads; *F*). Nontransfected cells stimulated with IGF-I demonstrate expression of E-cadherin (red; *G*), rab5 immunoreactivity (green; *H*), and their colocalization (yellow and arrowheads; *I*). Scale bar, 5 μm. *J*: total and subcellular fractionated protein extracted from IGF-I-stimulated mIMCD3 cells were subjected to Western blot analysis. Although there was no change in total cell β-catenin content, IGF stimulation resulted in rapid translocation of β-catenin to the nucleus. *K*: total cell protein extracted from cells stimulated with IGF-I or TGF-β1 for 1 and 72 h, immunoprecipitated (IP) with E-cadherin antibodies, and then immunoblotted with β-catenin antibodies demonstrated a decrease in expression of β-catenin in stimulated cells, suggesting a dissociation of E-cadherin-β-catenin complexes.

MAP kinase pathway activation, as demonstrated by an increase in Erk1/2 phosphorylation as early as 15 min, persisting to at least 1 h of TGF-β1 stimulation (Fig. 5*B*).

Coincubation of IGF-I and TGF-β1. We next analyzed the effect of coincubation of IGF-I and TGF-β1 on intracellular signaling. Although we observed an increase in Smad3 phosphorylation compared with control cells, costimulation with TGF-β1 and IGF-I for up to 3 h resulted in a significant reduction in Smad3 phosphorylation compared with TGF-β1-stimulated cells, with a maximum 1.5-fold increase at 15 min (Fig. 7) compared with a 3-fold increase in cells stimulated with TGF-β1 alone (Fig. 5*B*). As with Smad3, coincubation of IGF-I and TGF-β1 resulted in a decrease in early Akt phosphorylation compared with IGF-I stimulation alone, with a maximum twofold increase (Fig. 7) compared with an approximately threefold increase with IGF-I stimulation alone (Fig. 5*A*). Costimulation of the mIMCD3 cell monolayers did not result in any significant Erk1/2 phosphorylation at either early or late time points, in contrast to the significant early activation by TGF-β1 alone (Fig. 5*B*). The effect of IGF-I and TGF-β1 coincubation on GSK-3β at early time points was similar to that seen with Smad3 and Akt, with a blunting of rapid phosphorylation but no significant changes compared with unstimulated control cells at later time points (Fig. 7).

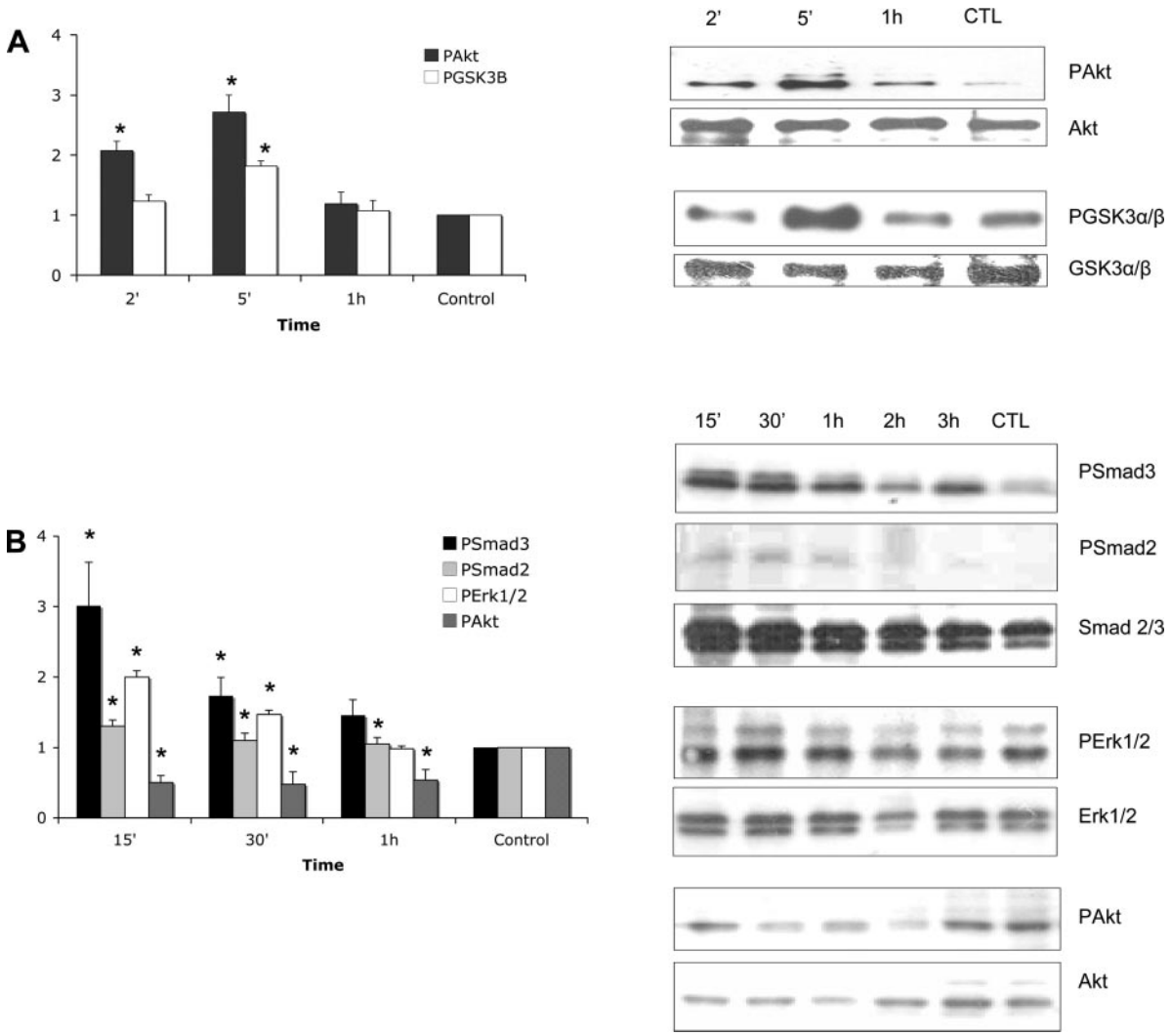

Fig. 5. Early cell signaling in stimulated mIMCD3 cells. *A*: mIMCD3 cells were stimulated with IGF-I (10 ng/ml), and total cell protein was extracted and analyzed by Western blot for intracellular pathway activation and compared with control unstimulated cells grown under identical conditions. IGF-I stimulation resulted in a significant increase in phosphorylated (p)Akt expression to 5 min and a significant increase in glycogen synthetase kinase (GSK)-3β phosphorylation at 5 min compared with control, unstimulated cells (CTL). Data are presented as means ± SE ($n = 3$ experiments), with corresponding representative Western blots. Values for phosphorylated protein are corrected for total protein of the same species. *$P < 0.05$ vs. control. *B*: mIMCD3 cells were similarly stimulated with TGF-β1 (10 ng/ml) and compared with control unstimulated cells grown under identical conditions. TGF-β1 stimulation resulted in a significant increase in phosphorylated Smad3 to 30 min and Smad2 expression to 1 h, a significant increase in Erk1/2 phosphorylation to 30 min, and a significant decrease in Akt phosphorylation to at least 1 h after stimulation compared with control, unstimulated cells. Data are presented as means ± SE ($n = 3$ experiments), with corresponding representative Western blots. Values for phosphorylated protein are corrected for total protein of the same species. *$P < 0.05$ vs. control.

Upregulation of Snail. We next studied the effects of IGF stimulation on the expression of Snail in mIMCD3 cells. Snail is a transcription factor that promotes epithelial-to-mesenchymal transitions during development (47), and while it has been implicated in obstructive nephropathy, its role in CD EMT has not been described. Snail demonstrated only low-level cytoplasmic expression in unstimulated control mIMCD3 cells under serum-free conditions (Fig. 8*A*). Stimulation of cells with IGF-I and with TGF-β1 for 30 min resulted in an increase in both nuclear and cytoplasmic Snail1 expression, as demonstrated by immunohistochemistry and by Western blot analysis (Fig. 8, *B–D*). Interestingly, at 72 h of incubation Snail was upregulated only in TGF-β1-stimulated cells (Fig. 8*E*).

Effect of Smad3 inhibition on TGF-β1-mediated EMT in mIMCD3 cells. Recently SIS3 has been shown to selectively suppress Smad3 phosphorylation, thereby abolishing the overexpression of matrix proteins in TGF-β1-treated dermal fibroblasts in vitro (20). Therefore, to help define the role of Smad3 phosphorylation in TGF-β1-induced CD EMT, we preincubated cells with SIS3 before stimulation. Treatment with SIS3 resulted in suppression of baseline Smad3 phosphorylation in unstimulated cells in a dose-dependent manner, whereas the expression of total protein was unaffected (data not shown). Pretreatment of mIMCD3 cells with 1 μM SIS3 for 30 min before stimulation with TGF-β1 markedly decreased Smad3 phosphorylation (Fig. 9*A*). SIS3 did not result in Erk or Akt phosphorylation in control or TGF-β1-treated IMCD3 cells (data not shown). Next we evaluated the effect of SIS3 on E-cadherin, β-catenin, and SMA expression in TGF-β1-stimulated cells. Pretreatment of mIMCD3 cells with 1 μM SIS3 for 30 min before TGF-β1 stimulation for 72 h resulted in lower SMA and higher E-cadherin and β-catenin expression

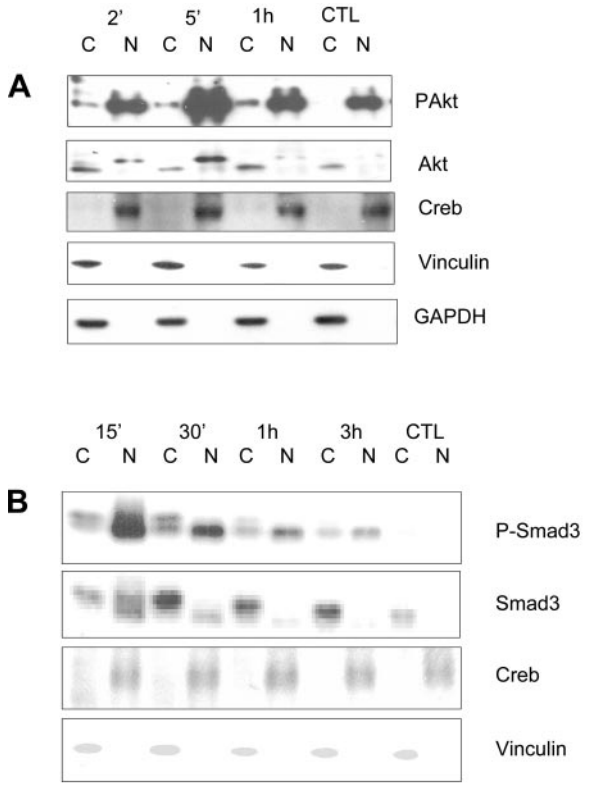

Fig. 6. Nuclear translocation of phosphorylated Akt and Smad3. *A*: mIMCD3 cells stimulated with IGF-I (10 ng/ml) showed a rapid increase in phosphorylated Akt both in the cytoplasmic (C) and nuclear (N) cell compartments as early as 2 min after stimulation. *B*: cells stimulated with TGF-β1 (10 ng/ml) showed a similar rapid distribution of phosphorylated Smad3 expression to the nuclear and cytoplasmic compartments as early as 15 min after stimulation.

levels compared with TGF-β1 treatment alone (Fig. 9*B*). Analysis of cell immunoreactivity by fluorescence microscopy was consistent with Western blot analysis of whole cell protein, indicating a persistence of de novo SMA expression in SIS3-pretreated cells (Fig. 9, *C* and *D*). As shown, TGF-β1 treatment resulted in a reduction of E-cadherin and β-catenin protein as well as a dissociation of the E-cadherin-β-catenin contacts (Fig. 9*E*); however, pretreatment of cells with SIS3 protected the integrity of basolateral distribution and colocalization of both adherens junction proteins (Fig. 9*F*). These results suggest that SIS3 attenuates TGF-β1-mediated EMT in mIMCD3 cells by selectively reducing Smad3 phosphorylation, and by preventing the dislocation and downregulation of the junctional proteins E-cadherin and β-catenin.

Effect of PI3-kinase inhibition on IGF-I-mediated EMT in mIMCD3 cells. Our results show that IGF-I-induced EMT in mIMCD3 cells is associated with rapid Akt phosphorylation and activation (Figs. 5*A*, 6*A*). To directly examine the role of PI3-kinase pathway activation in IGF-I-induced CD EMT, we determined the effect of preincubation of the cells with the PI3-kinase inhibitor LY-294002 (20 μM) before IGF stimulation. Western blot analysis demonstrated downregulation of Akt activation by LY-294002 in IGF-I-stimulated cells (Fig. 10*A*). mIMCD3 cells were pretreated with LY-294002 and then incubated with IGF-I for 72 h. Western blot analysis revealed little change in the amount of E-cadherin and SMA expression; however, β-catenin expression was increased compared with cells not pretreated with inhibitor (Fig. 10*B*). As before, by immunohistochemistry IGF-I-stimulated cells displayed prominent SMA expression in stress fibers (Fig. 10*C*). While preincubation with LY-294002 did not inhibit de novo SMA expression, its distribution was diffuse and throughout the cell cytoplasm rather than restricted to cytoskeletal stress fibers (Fig. 10*D*). In IGF-I-stimulated cells there was loss of colocalization of E-cadherin and β-catenin at the cell membrane adherens junctions, with displacement of E-cadherin to cytoplasmic endosomes and of β-catenin to the nucleus (Fig. 10*E*). With inhibition of PI3-kinase activation, these IGF-I-induced effects were attenuated, with preservation of membrane localization of β-catenin and colocalization of E-cadherin and β-catenin at the cell junctions (Fig. 10*F*).

DISCUSSION

In this study we have demonstrated the ability of a CD cell line to undergo EMT with stimulation by IGF-I, by TGF-β1, and by a combination of the two factors. A number of investigators have reproduced this phenotypic transition in vivo in proximal tubular epithelial cells of obstructed mouse kidneys and in vitro in proximal tubule epithelial cells stimulated by various profibrotic agents such as TGF-β1 (34, 56, 57). This to our knowledge is the first report of the ability of CD cells to undergo EMT in vitro, and it supports our previous observations (7) of this phenomenon in vivo in a fetal monkey model of urinary tract obstruction.

The role of IGF-I in tissue fibrosis is largely unknown, with conflicting reports of salutary effects of the peptide and no effects of its inhibition in experimental urinary tract obstruction (8, 38). We previously demonstrated (29) overexpression of IGFs in the expanded interstitium of dysplastic fetal kidneys, suggesting a profibrotic role for this peptide in fetal urinary tract obstruction and in renal dysplasia. In vitro, however, IGF has been shown to directly induce EMT, through disruption of cell membrane cadherin-catenin complexes in rat

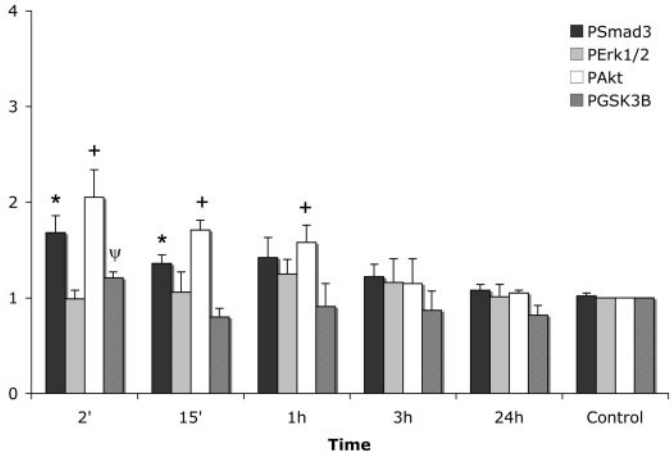

Fig. 7. Modulation of IGF-I signaling by TGF-β1 in mIMCD3 cells. Western blot analyses of cells stimulated with IGF-I (10 ng/ml) and TGF-β1 (10 ng/ml) demonstrate a significant increase in Smad3 phosphorylation as early as 2 min that persists up to 15 min of stimulation, a significant increase in Akt phosphorylation as early as 2 min that persists up to 1 h of stimulation, and a significant increase in GSK-3β phosphorylation at 2 min, with no significant increase in Erk1/2 phosphorylation compared with control, unstimulated cells. Data are presented as means ± SE ($n = 3$ experiments). *+Ψ$P < 0.05$ vs. control.

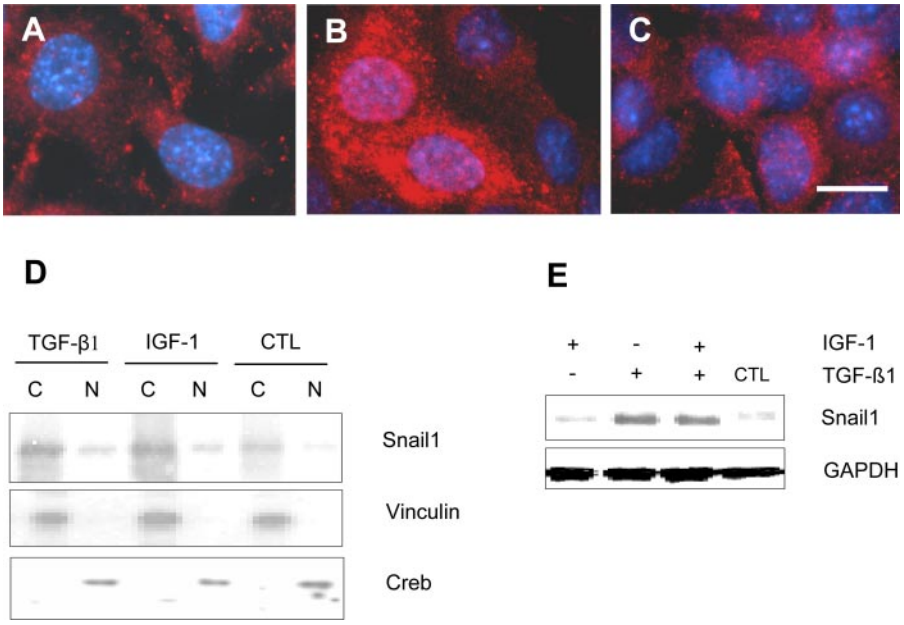

Fig. 8. Induction of Snail1 expression. *A*: in control, unstimulated cells there was minimal cytoplasmic expression of Snail1. *B*: cells stimulated with IGF-I for 30 min showed rapid increases in both cytoplasmic and nuclear expression of Snail1, with a similar response to TGF-β1 (10 ng/ml; *C*). Scale bar, 10 μm. *D*: Western blot analysis of fractionated cell protein showing an increase in both nuclear and cytoplasmic Snail1 protein expression with IGF-I and TGF-β1 stimulation at 30 min, consistent with results of immunohistochemistry. *E*: After 72 h Snail1 expression was increased only in cells stimulated with TGF-β1.

bladder carcinoma (NBT-II) and human mammary carcinoma (MCF-7) cell lines (33), through upregulation of the connective tissue growth factor CCN6 in human mammary epithelial (HME) cells (58), and most recently through the activation of the transcription factors NF-κB and Snail in the mammary epithelial cell line MCF-10A (23). In this study we demonstrated the ability of IGF-I to induce mesenchymal transformation in CD epithelial cells. IGF-I stimulation of mIMCD3 cells resulted in activation of the PI3-kinase pathway, with rapid Akt and GSK-3β phosphorylation, Akt translocation to the nucleus, and early upregulation of Snail1, but without demonstrable Smad3 or MAP kinase pathway activation. The late consequences of this stimulation are the phenotypic and morphological transformation of the cells and the upregulation

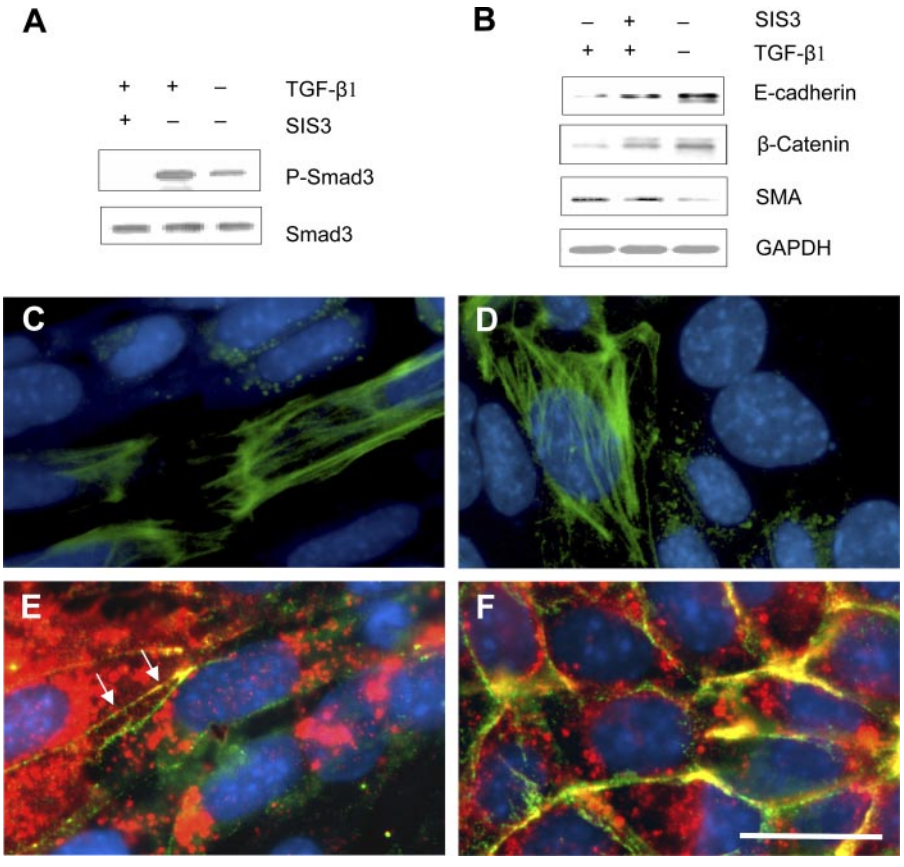

Fig. 9. Effects of inhibition of TGF-β1 signaling. *A*: pretreatment of cells with specific inhibitor of Smad3 (SIS3, 1 μM) inhibited TGF-β1-stimulated Smad3 phosphorylation after 30 min. *B*: Western blot analysis of total protein from cells stimulated with TGF-β1 for 72 h and pretreated with SIS3, demonstrating an increase in E-cadherin and β-catenin expression, with no change in SMA expression, compared with TGF-β1-stimulated cells. TGF-β1-stimulated cells display an increase in SMA expression (green; *C*), while preincubation with SIS3 does not alter TGF-β1 effects on SMA expression (*D*). While TGF-β1-stimulated cells display dislocated E-cadherin (red) from the cell membrane to cytoplasmic endosomes (*E*), β-catenin (green) continues to be expressed at the cell membrane (arrows) *F*: Cells incubated with SIS3 maintained their expression of E-cadherin at the cell membrane, where it colocalized with β-catenin (yellow). Scale bar, 10 μm.

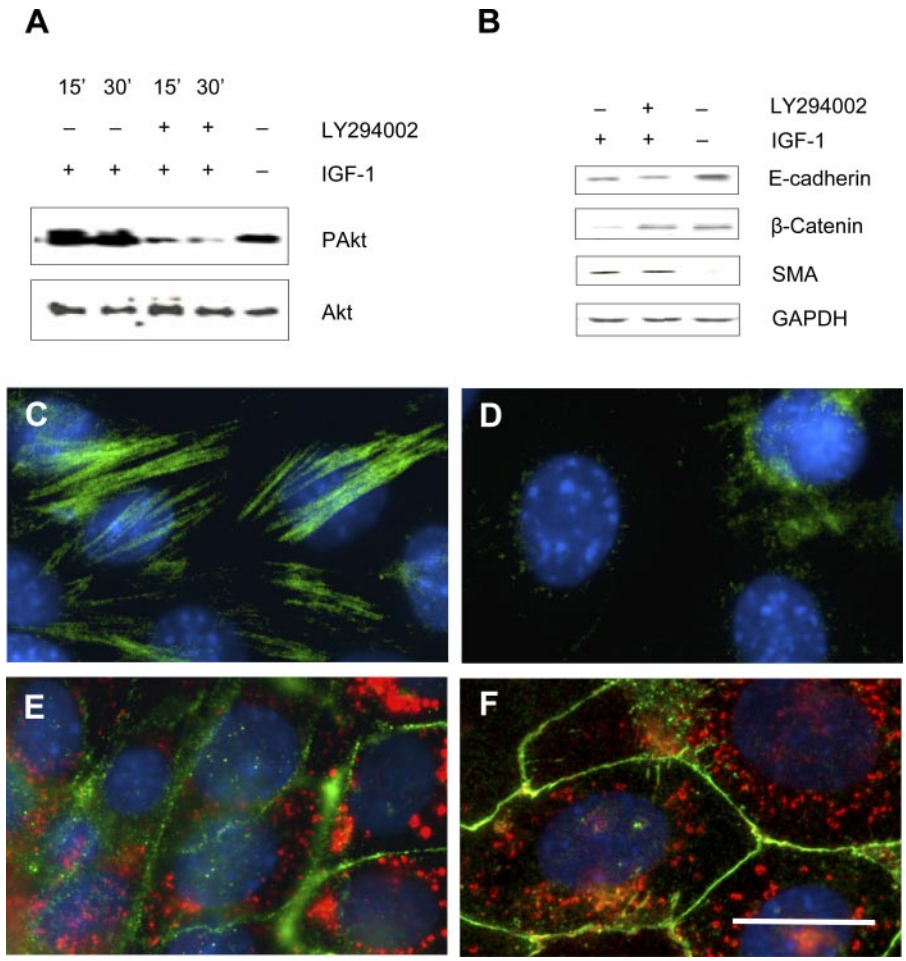

Fig. 10. Effects of inhibition of IGF-I signaling. *A*: coincubation of cells with LY-294002 (20 μM) inhibited IGF-I-stimulated Akt phosphorylation after 15 min. *B*: Western blot analysis of total protein from cells stimulated with IGF-I for 72 h in the presence of LY-294002, demonstrating an increase in β-catenin expression, with little change in the total cell content of E-cadherin and SMA, compared with IGF-I-stimulated cells without inhibitor. *C*: IGF-I-stimulated cells display an increase in SMA expression (green) after 72 h. *D*: inhibition of Akt phosphorylation by coincubation with LY-294002 abrogated the increase in IGF-stimulated SMA expression. *E*: cells stimulated with IGF-I for 72 h display dislocated E-cadherin (red) and β-catenin (green) from the cell membrane. *F*: cells incubated with LY-294002 continued to express predominantly β-catenin at the cell membrane (green). Scale bar, 10 μm.

of SMA and vimentin expression. These late consequences are likely mediated in part through the effects of nuclear import of Akt, GSK-3β, Snail, and possibly β-catenin on the transcription of EMT genes (21). While IGF appeared to increase β-catenin translocation to the nucleus in these experiments, it may have also directly affected the stability of cytoplasmic levels of β-catenin through phosphorylation by GSK-3β, shown to be activated rapidly after IGF stimulation in these cells (15, 33).

Phenotypic transition stimulated by TGF-β1, on the other hand, has been defined in a number of cell types and appears to be mediated predominantly through Smad signaling (16, 46). As expected in our cell system, TGF-β1 stimulation resulted in early Smad3, and to a lesser extent Smad2, phosphorylation and translocation to the nucleus, upregulation of Snail1, as well as an early activation of the MAP kinase pathway. The late effects of this early Smad3 nuclear import and Erk1/2 phosphorylation appear to be the upregulation of SMA and vimentin gene transcription and protein translation. Recent evidence suggests that Smad2 and Smad3 have distinct roles in TGF-β1-induced cellular responses (13, 24) because of very different effects on gene transcription (39, 40) due to differences in DNA-binding ability. Selective knockdown of Smad2 and Smad3 in kidney proximal tubule epithelial cells (PTECs) has shown Smad3-dependent increases in TGF-β1-induced connective tissue growth factor (CTGF) and decreases in E-cadherin expression, whereas increases in matrix metalloproteinase (MMP)-2 expression were Smad2 dependent (39).

In these experiments and over the course of mIMCD3 EMT, we have noted a dramatic disruption of cell junctions. This disruption of adherens junctions induced both by IGF-I and by TGF-β1 are relatively early processes compared with the repression of E-cadherin gene transcription and new protein translation. Our results show that the alteration in expression of total cellular E-cadherin protein during EMT in mIMCD3 cells was much slower (24–72 h) than the dislocation of E-cadherin from the cell junction to cytoplasmic vesicles (3 h) and that these growth factor-induced effects are early and immediate and may be mediated by endocytosis. In fact, in confluent Madin-Darby canine kidney (MDCK) cell monolayers at steady state a pool of surface E-cadherin remains subject to endocytosis and is recycled to the cell surface (53). E-cadherin endocytosis via a clathrin-mediated pathway and subsequent recycling to the surface has also been described (17). The precise mechanism for this disruption of membrane cadherin-catenin complexes in our cells is unknown; however, interestingly, both E-cadherin and β-catenin have consensus serine/threonine or tyrosine phosphorylation sites that have been shown to play a role in cellular adhesion (45) and are potential signaling targets of multiple protein kinases that have been implicated in E-cadherin trafficking, its endocytosis, and its recycling (4, 22, 25, 48). In this study we observed significant

activation of ERK1/2 kinases on stimulation by TGF-β1 and of PI3-kinase by IGF-I. When Smad3 phosphorylation was inhibited in our cell model, TGF-β1-induced EMT was attenuated and early translocation of E-cadherin from the cell membrane was abrogated. When PI3-kinase activation was inhibited, IGF-I-induced EMT was also attenuated but was associated with the maintenance of membrane colocalization of both β-catenin and E-cadherin. These results suggest a role for early intracellular signaling in the disruption of membrane cadherin-catenin complex integrity in mIMCD3 cells. Similarly, activation of the MEK1-ERK1/2 signaling module has been shown to induce EMT in renal epithelial MDCK-C7 cells (48), while activation of p42/p44 MAPK, PI3-kinase,and Rac downstream of Ras is required for hepatocyte growth factor (HGF)/scatter factor (SF)-induced disruption of adherens junctions (41).

In summary, we have demonstrated the ability of both IGF-I and TGF-β1 to induce EMT in a cell model system of the CD epithelium. While the mechanism appears complex, early events include disruption of cadherin-catenin complexes whereas late events mediated by the nuclear translocation of activated kinases, the stabilization of β-catenin, and Snail include a downregulation of cadherin expression and an upregulation of mesenchymal proteins including actin and vimentin.

GRANTS

This work was supported by a grant from the Kidney Foundation of Canada (D. G. Matsell).

REFERENCES

1. **Bates RC, Pursell BM, Mercurio AM.** Epithelial-mesenchymal transition and colorectal cancer: gaining insights into tumor progression using LIM 1863 cells. *Cells Tissues Organs* 185: 29–39, 2007.
2. **Bentov I, Werner H.** IGF, IGF receptor and overgrowth syndromes. *Pediatr Endocrinol Rev* 1: 352–360, 2004.
3. **Bottinger EP.** TGF-beta in renal injury and disease. *Semin Nephrol* 27: 309–320, 2007.
4. **Braga VM, Del Maschio A, Machesky L, Dejana E.** Regulation of cadherin function by Rho and Rac: modulation by junction maturation and cellular context. *Mol Biol Cell* 10: 9–22, 1999.
5. **Bridgewater DJ, Dionne JM, Butt MJ, Pin CL, Matsell DG.** The role of the type I insulin-like growth factor receptor (IGF-IR) in glomerular integrity. *Growth Horm IGF Res* 22: 222–223, 2007.
6. **Bridgewater DJ, Ho J, Sauro V, Matsell DG.** Insulin-like growth factors inhibit podocyte apoptosis through the PI3 kinase pathway. *Kidney Int* 67: 1308–1314, 2005.
7. **Butt MJ, Tarantal AF, Jimenez DF, Matsell DG.** Collecting duct epithelial-mesenchymal transition in fetal urinary tract obstruction. *Kidney Int* 72: 936–944, 2007.
8. **Chevalier RL, Goyal S, Kim A, Chang AY, Landau D, LeRoith D.** Renal tubulointerstitial injury from ureteral obstruction in the neonatal rat is attenuated by IGF-1. *Kidney Int* 57: 882–890, 2000.
9. **Devon RS, Orban PC, Gerrow K, Barbieri MA, Schwab C, Cao LP, Helm JR, Bissada N, Cruz-Aguado R, Davidson TL, Witmer J, Metzler M, Lam CK, Tetzlaff W, Simpson EM, McCaffery JM, El-Husseini AE, Leavitt BR, Hayden MR.** Als2-deficient mice exhibit disturbances in endosome trafficking associated with motor behavioral abnormalities. *Proc Natl Acad Sci USA* 103: 9595–9600, 2006.
10. **Dignam JD, Martin PL, Shastry BS, Roeder RG.** Eukaryotic gene transcription with purified components. *Methods Enzymol* 101: 582–598, 1983.
11. **Eddy AA.** Experimental insights into the tubulointerstitial disease accompanying primary glomerular lesions. *J Am Soc Nephrol* 5: 1273–1287, 1994.
12. **Essawy M, Soylemezoglu O, Muchaneta-Kubara EC, Shortland J, Brown CB, el Nahas AM.** Myofibroblasts and the progression of diabetic nephropathy. *Nephrol Dial Transplant* 12: 43–50, 1997.
13. **Flanders KC.** Smad3 as a mediator of the fibrotic response. *Int J Exp Pathol* 85: 47–64, 2004.
14. **Hartsock A, Nelson WJ.** Adherens and tight junctions: Structure, function and connections to the actin cytoskeleton. *Biochim Biophys Acta* 22: 22–223, 2007.
15. **He X.** A Wnt-Wnt situation. *Dev Cell* 4: 791–797, 2003.
16. **Inazaki K, Kanamaru Y, Kojima Y, Sueyoshi N, Okumura K, Kaneko K, Yamashiro Y, Ogawa H, Nakao A.** Smad3 deficiency attenuates renal fibrosis, inflammation, and apoptosis after unilateral ureteral obstruction. *Kidney Int* 66: 597–604, 2004.
17. **Ivanov AI, Nusrat A, Parkos CA.** Endocytosis of epithelial apical junctional proteins by a clathrin-mediated pathway into a unique storage compartment. *Mol Biol Cell* 15: 176–188, 2004.
18. **Iwano M, Plieth D, Danoff TM, Xue C, Okada H, Neilson EG.** Evidence that fibroblasts derive from epithelium during tissue fibrosis. *J Clin Invest* 110: 341–350, 2002.
19. **Jinde K, Nikolic-Paterson DJ, Huang XR, Sakai H, Kurokawa K, Atkins RC, Lan HY.** Tubular phenotypic change in progressive tubulointerstitial fibrosis in human glomerulonephritis. *Am J Kidney Dis* 38: 761–769, 2001.
20. **Jinnin M, Ihn H, Tamaki K.** Characterization of SIS3, a novel specific inhibitor of Smad3, and its effect on transforming growth factor-beta1-induced extracellular matrix expression. *Mol Pharmacol* 69: 597–607, 2006.
21. **Kalluri R, Neilson EG.** Epithelial-mesenchymal transition and its implications for fibrosis. *J Clin Invest* 112: 1776–1784, 2003.
22. **Kamei T, Matozaki T, Sakisaka T, Kodama A, Yokoyama S, Peng YF, Nakano K, Takaishi K, Takai Y.** Coendocytosis of cadherin and c-Met coupled to disruption of cell-cell adhesion in MDCK cells—regulation by Rho, Rac and Rab small G proteins. *Oncogene* 18: 6776–6784, 1999.
23. **Kim HJ, Litzenburger BC, Cui X, Delgado DA, Grabiner BC, Lin X, Lewis MT, Gottardis MM, Wong TW, Attar RM, Carboni JM, Lee AV.** Constitutively active type I insulin-like growth factor receptor causes transformation and xenograft growth of immortalized mammary epithelial cells and is accompanied by an epithelial-to-mesenchymal transition mediated by NF-kappaB and snail. *Mol Cell Biol* 27: 3165–3175, 2007.
24. **Kretschmer A, Moepert K, Dames S, Sternberger M, Kaufmann J, Klippel A.** Differential regulation of TGF-beta signaling through Smad2, Smad3 and Smad4. *Oncogene* 22: 6748–6763, 2003.
25. **Le TL, Joseph SR, Yap AS, Stow JL.** Protein kinase C regulates endocytosis and recycling of E-cadherin. *Am J Physiol Cell Physiol* 283: C489–C499, 2002.
26. **Liu Y.** Renal fibrosis: new insights into the pathogenesis and therapeutics. *Kidney Int* 69: 213–217, 2006.
27. **Lopes JA, Moreso F, Riera L, Carrera M, Ibernon M, Fulladosa X, Grinyo JM, Seron D.** Evaluation of pre-implantation kidney biopsies: comparison of Banff criteria to a morphometric approach. *Kidney Int* 67: 1595–1600, 2005.
28. **Matsell DG.** Renal dysplasia: new approaches to an old problem. *Am J Kidney Dis* 32: 535–543, 1998.
29. **Matsell DG, Bennett T, Armstrong RA, Goodyer P, Goodyer C, Han VK.** Insulin-like growth factor (IGF) and IGF binding protein gene expression in multicystic renal dysplasia. *J Am Soc Nephrol* 8: 85–94, 1997.
30. **Matsell DG, Bennett T, Goodyer P, Goodyer C, Han VK.** The pathogenesis of multicystic dysplastic kidney disease: insights from the study of fetal kidneys. *Lab Invest* 74: 883–893, 1996.
31. **Matsell DG, Delhanty PJ, Stepaniuk O, Goodyear C, Han VK.** Expression of insulin-like growth factor and binding protein genes during nephrogenesis. *Kidney Int* 46: 1031–1042, 1994.
32. **Mohammed JA, Mok AY, Parbtani A, Matsell DG.** Increased expression of insulin-like growth factors in progressive glomerulonephritis of the MRL/lpr mouse. *Lupus* 12: 584–590, 2003.
33. **Morali OG, Delmas V, Moore R, Jeanney C, Thiery JP, Larue L.** IGF-II induces rapid beta-catenin relocation to the nucleus during epithelium to mesenchyme transition. *Oncogene* 20: 4942–4950, 2001.
34. **Morrissey J, Guo G, Moridaira K, Fitzgerald M, McCracken R, Tolley T, Klahr S.** Transforming growth factor-beta induces renal epithelial jagged-1 expression in fibrotic disease. *J Am Soc Nephrol* 13: 1499–1508, 2002.
35. **Nankivell BJ, Fenton-Lee CA, Kuypers DR, Cheung E, Allen RD, O'Connell PJ, Chapman JR.** Effect of histological damage on long-term kidney transplant outcome. *Transplantation* 71: 515–523, 2001.
36. **Negri AL.** Prevention of progressive fibrosis in chronic renal diseases: antifibrotic agents. *J Nephrol* 17: 496–503, 2004.

37. **Ng YY, Huang TP, Yang WC, Chen ZP, Yang AH, Mu W, Nikolic-Paterson DJ, Atkins RC, Lan HY.** Tubular epithelial-myofibroblast transdifferentiation in progressive tubulointerstitial fibrosis in 5/6 nephrectomized rats. *Kidney Int* 54: 864–876, 1998.
38. **Oldroyd SD, Miyamoto Y, Moir A, Johnson TS, El Nahas AM, Haylor JL.** An IGF-I antagonist does not inhibit renal fibrosis in the rat following subtotal nephrectomy. *Am J Physiol Renal Physiol* 290: F695–F702, 2006.
39. **Phanish MK, Wahab NA, Colville-Nash P, Hendry BM, Dockrell ME.** The differential role of Smad2 and Smad3 in the regulation of pro-fibrotic TGFbeta1 responses in human proximal-tubule epithelial cells. *Biochem J* 393: 601–607, 2006.
40. **Piek E, Ju WJ, Heyer J, Escalante-Alcalde D, Stewart CL, Weinstein M, Deng C, Kucherlapati R, Bottinger EP, Roberts AB.** Functional characterization of transforming growth factor beta signaling in Smad2- and Smad3-deficient fibroblasts. *J Biol Chem* 276: 19945–19953, 2001.
41. **Potempa S, Ridley AJ.** Activation of both MAP kinase and phosphatidylinositide 3-kinase by Ras is required for hepatocyte growth factor/scatter factor-induced adherens junction disassembly. *Mol Biol Cell* 9: 2185–2200, 1998.
42. **Rastaldi MP, Ferrario F, Giardino L, Dell'Antonio G, Grillo C, Grillo P, Strutz F, Muller GA, Colasanti G, D'Amico G.** Epithelial-mesenchymal transition of tubular epithelial cells in human renal biopsies. *Kidney Int* 62: 137–146, 2002.
43. **Rauchman MI, Nigam SK, Delpire E, Gullans SR.** An osmotically tolerant inner medullary collecting duct cell line from an SV40 transgenic mouse. *Am J Physiol Renal Fluid Electrolyte Physiol* 265: F416–F424, 1993.
44. **Rocha KB, Soares VA, Viero RM.** The role of myofibroblasts and interstitial fibrosis in the progression of membranous nephropathy. *Ren Fail* 26: 445–451, 2004.
45. **Roura S, Miravet S, Piedra J, Garcia de Herreros A, Dunach M.** Regulation of E-cadherin/catenin association by tyrosine phosphorylation. *J Biol Chem* 274: 36734–36740, 1999.
46. **Sato M, Muragaki Y, Saika S, Roberts AB, Ooshima A.** Targeted disruption of TGF-beta1/Smad3 signaling protects against renal tubulointerstitial fibrosis induced by unilateral ureteral obstruction. *J Clin Invest* 112: 1486–1494, 2003.
47. **Schlessinger K, Hall A.** GSK-3beta sets Snail's pace. *Nat Cell Biol* 6: 913–915, 2004.
48. **Schramek H, Feifel E, Marschitz I, Golochtchapova N, Gstraunthaler G, Montesano R.** Loss of active MEK1-ERK1/2 restores epithelial phenotype and morphogenesis in transdifferentiated MDCK cells. *Am J Physiol Cell Physiol* 285: C652–C661, 2003.
49. **Selgas R, Bajo A, Jimenez-Heffernan JA, Sanchez-Tomero JA, Del Peso G, Aguilera A, Lopez-Cabrera M.** Epithelial-to-mesenchymal transition of the mesothelial cell—its role in the response of the peritoneum to dialysis. *Nephrol Dial Transplant* 21, *Suppl* 2: ii2–ii7, 2006.
50. **Striker GE, Peten EP, Yang CW, Striker LJ.** Glomerulosclerosis: studies of its pathogenesis in humans and animals. *Contrib Nephrol* 107: 124–131, 1994.
51. **Tack I, Elliot SJ, Potier M, Rivera A, Striker GE, Striker LJ.** Autocrine activation of the IGF-I signaling pathway in mesangial cells isolated from diabetic NOD mice. *Diabetes* 51: 182–188, 2002.
52. **Tarantal AF, Han VK, Cochrum KC, Mok A, daSilva M, Matsell DG.** Fetal rhesus monkey model of obstructive renal dysplasia. *Kidney Int* 59: 446–456, 2001.
53. **Vogelmann R, Nguyen-Tat MD, Giehl K, Adler G, Wedlich D, Menke A.** TGFbeta-induced downregulation of E-cadherin-based cell-cell adhesion depends on PI3-kinase and PTEN. *J Cell Sci* 118: 4901–4912, 2005.
54. **Vongwiwatana A, Tasanarong A, Rayner DC, Melk A, Halloran PF.** Epithelial to mesenchymal transition during late deterioration of human kidney transplants: the role of tubular cells in fibrogenesis. *Am J Transplant* 5: 1367–1374, 2005.
55. **Willis BC, Borok Z.** TGF-β-induced EMT: mechanisms and implications for fibrotic lung disease. *Am J Physiol Lung Cell Mol Physiol* 293: L525–L534, 2007.
56. **Yang J, Liu Y.** Dissection of key events in tubular epithelial to myofibroblast transition and its implications in renal interstitial fibrosis. *Am J Pathol* 159: 1465–1475, 2001.
57. **Zeisberg M, Hanai J, Sugimoto H, Mammoto T, Charytan D, Strutz F, Kalluri R.** BMP-7 counteracts TGF-beta1-induced epithelial-to-mesenchymal transition and reverses chronic renal injury. *Nat Med* 9: 964–968, 2003.
58. **Zhang Y, Pan Q, Zhong H, Merajver SD, Kleer CG.** Inhibition of CCN6 (WISP3) expression promotes neoplastic progression and enhances the effects of insulin-like growth factor-1 on breast epithelial cells. *Breast Cancer Res* 7: R1080–1089, 2005.